ORIGIN OF THE SOLAR WIND FROM COMPOSITION DATA

J. GEISS
Physikalisches Institut, University of Bern, Sidlerstrasse 5, CH–3012 Bern, Switzerland

G. GLOECKLER
Department of Physics and Astronomy, University of Maryland, College Park, MD 20742, USA

and

R. VON STEIGER
Physikalisches Institut, University of Bern, Sidlerstrasse 5, CH–3012 Bern, Switzerland

Abstract. The ESA/NASA spacecraft Ulysses is making, for the first time, direct measurements in the solar wind originating from virtually all places where the corona expands. Since the initial two polar passes of Ulysses occur during relatively quiet solar conditions, we discuss here the three main regimes of quasi-stationary solar wind flow: the high speed streams (HSSTs) coming out of the polar coronal holes, the slow solar wind surrounding the HSSTs, and the streamers which occur at B-field reversals. Comparisons between H-α maps and data taken by Ulysses demonstrate that as a result of super-radial expansion, the HSSTs occupy a much larger solid angle than that derived from radial projections of coronal holes. Data obtained with SWICS-Ulysses confirm that the strength of the FIP effect is much reduced in the HSSTs. The systematics in the variations of elemental abundances becomes particularly clear, if these are plotted against the time of ionisation (at the solar surface) rather than against the first ionisation potential (FIP). We have used a superposed-epoch method to investigate the changes in solar wind speed and composition measured during the 9-month period in 1992/93 when Ulysses regularly passed into and out of the southern HSST. We find that the patterns in the variations of the Mg/O and O^{7+}/O^{6+} ratios are virtually identical and that their transition from high to low values is very steep. Since the Mg/O ratio is controlled by the FIP effect and the O^{7+}/O^{6+} ratio reflects the coronal temperature, this finding points to a connection between chromospheric and coronal conditions.

1. Introduction

The source of the solar wind (SW) is the outer convective zone (OCZ) of the sun which is a large and well-mixed reservoir with a composition that remains stable over millions of years. Significant changes in composition are produced in the transport of solar matter from the OCZ to the corona, and in the process of lifting the coronal plasma out of the Sun's gravitational field. The question of the "origin of the solar wind" would be solved, if the ways and means of supplying matter, momentum and energy to corona and SW were quantitatively specified. Since Parker (1960, 1963) showed that under a broad range of physical conditions the solar corona expands into a supersonic outflow, the solar wind and – to a lesser extend – its composition have been experimentally investigated in considerable depth, leading to an understanding of many aspects of the dynamics of coronal expansion. However, we do not yet have a self consistent theory of material transport, coronal heating and solar wind acceleration, which reproduces the major observations of the flow of matter, momentum and energy, explaining at the same time the observed ion composition.

Space Science Reviews **72**: 49–60.

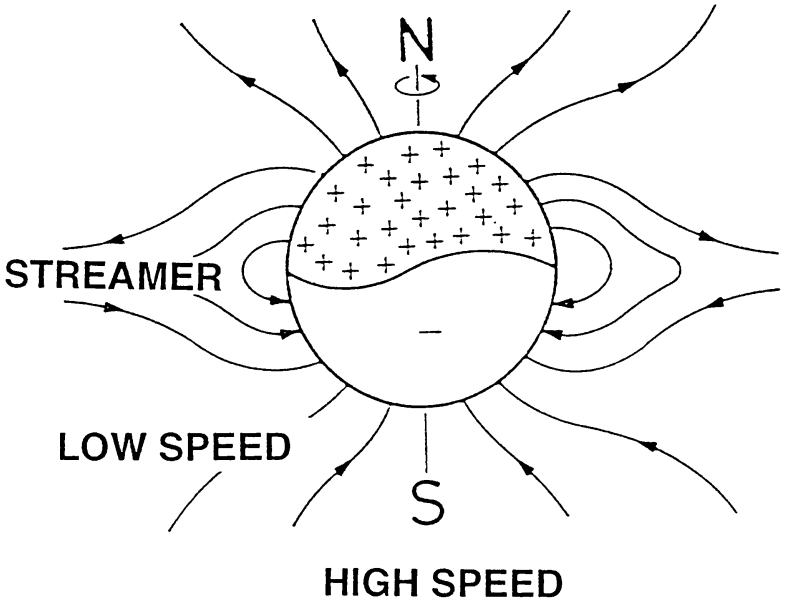

Fig. 1. Sketch of steady state solar wind expansion with dipole-type geometry.

Transient phenomena in the solar wind are often the rule rather than the exception. Is it then that the picture of a quiet SW is inappropriate and steady state theories are of questionable use even as an approximation? Observations show us that this is not the case: The solar wind never disappeared during the three decades it has been observed, and the flux variations were limited in range. In particular, in the 1970s the coronal holes were shown to emit high speed streams (HSSTs) (cf. Krieger et al., 1973) that were remarkably steady in their bulk properties and helium abundance (Bame et al., 1977). Since we approach now the solar minimum and since Ulysses' trajectory gives us the unique opportunity to study the solar wind at the high latitudes including the large HSSTs, we shall focus in this paper on the basic features of steady solar wind flow: The polar HSSTs, the slow SW surrounding it, and the streamers which occur at B-field reversals. More general and detailed accounts of the results of solar wind composition research are found in Neugebauer (1981), Schwenn and Marsch (1990), Geiss (1985), Bochsler and Geiss (1989), Gloeckler and Geiss (1989), and von Steiger and Geiss (1994).

A solar dipole field stretched out by the supersonic outflow (Fig. 1) is the simplest geometric configuration in which the three basic features of a steady SW flow can be described (cf. Hundhausen, 1972; Geiss and Bochsler, 1986). More complex geometries are often required for a realistic picture of the expansion (cf. Wang et al., 1993). However, for our discussion, the simple steady-state geometry we shown in Fig. 1 is a useful guide.

Models of coronal structure cannot be brought into agreement with the observations, unless the finite abundance of helium is taken into account (Noci and Porri, 1983). Thus a three-component plasma consisting of protons, alphas and electrons has to be used in corona expansion models, with the other ions treated as minor components (Bürgi and Geiss, 1986). Even before it enters the corona,

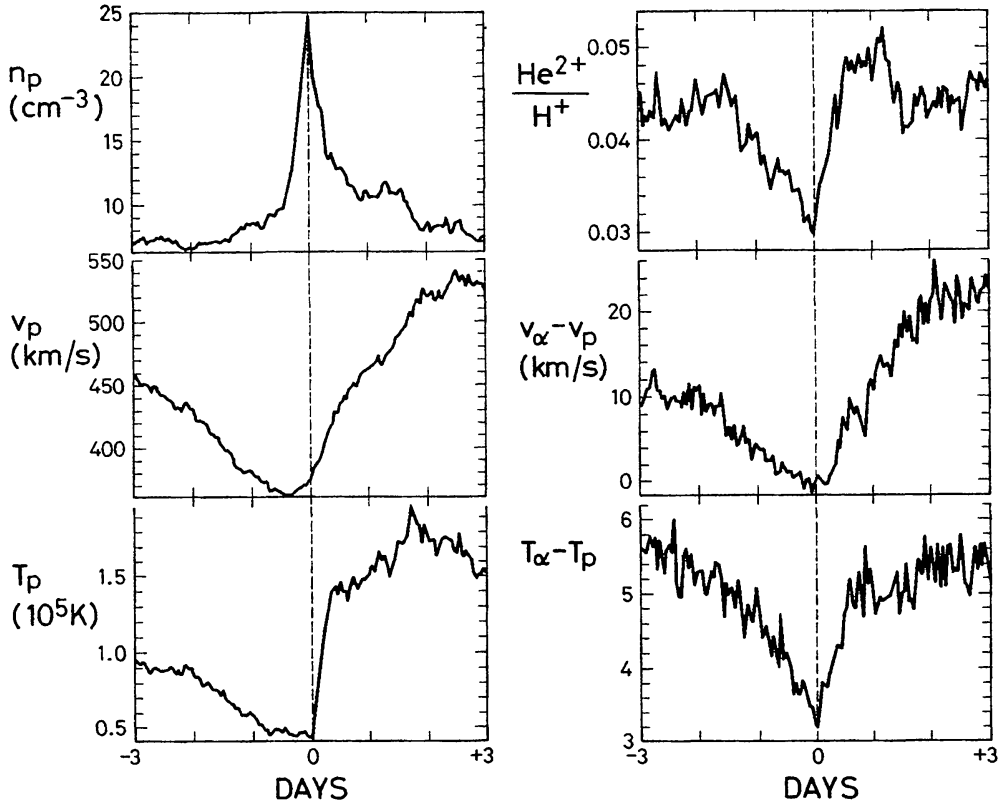

Fig. 2. Superposed epoch plots for 74 sector boundaries, showing a significant drop in the He/H ratio at the sector boundary, along with the characteristic changes of other solar wind parameters (from Borrini et al., 1981).

the solar gas is fractionated: Transport through the chromosphere into the corona causes an overabundance of elements with low first ionisation potential, the so called FIP-effect. Sofar, fractionation in the chromosphere has been considered independently from coronal heating and expansion. In this paper we present evidence for a causal connection.

2. The Slow Solar Wind in Streamers

There is a characteristic signature of the solar wind flow in the streamers, as has been demonstrated by Borrini et al. (1981) using the superposed epoch method (Fig. 2). Speed, kinetic temperature and He/H ratio have a minimum at the center of the current sheet which is identified by the B-field reversal. Schmid et al. (1988) found that also the iron abundance decreases near the B-field reversals. Although iron is much heavier than helium, the decrease for iron was not more pronounced than it was for helium. The reduced abundance of the heavier ions is – at least in part – due to the special B-field geometry: Near the sun, the expansion in streamers is probably supra-radial as Fig. 1 indicates, and consequently the SW speed there is exceptionally low allowing for gravitational de-mixing of helium and heavier ions from hydrogen. Bürgi (1992) has developed a model for

the expansion of a three-fluid (p-α-e) plasma and shows that in streamer-type geometries strong depletions of helium are indeed to be expected. It would be worthwhile to resume the studies pioneered by Borrini et al. (1981) and include some more solar wind parameters. If, for instance, the O^{6+} and O^{7+} abundances could be measured as a function of the distance from the field reversal, modelling of the streamer would be strongly constrained. The O^{7+}/O^{6+} would narrow the choice for the coronal temperature, and the O/He/H abundance ratio would give direct information on the expansion kinematics, as may be demonstrated by the following simple estimates.

The degree of demixing is governed by a competition between the speed of settling and the expansion speed (or a turbulent mixing parameter, as in the Earth's atmosphere). In an isothermal proton-electron plasma V_s, the speed of settling of a heavier ion (A, Z) under the influence of the solar gravity, the electric field and non-resonant momentum transfer from waves is given approximately as (cf. Geiss et al., 1970)

$$V_s = \text{const.}\,\frac{2A - Z - 1}{Z^2} \tag{1}$$

For the main ions of He and O, we obtain $V_s(He^{2+})/V_s(O^{6+}) = 1.8$. Thus if the settling speeds barely overcome the expansion speed, oxygen would be less depleted than helium.

The opposite is expected if expansion speed and/or turbulent mixing are so slow that a real gravitational stratification takes place. This can be seen from comparing the scale heights of the heavy ions (again for an isothermal proton-electron plasma)

$$H = \frac{kT}{m^\star g^\star} \tag{2}$$

where $g^\star$ is the local gravitational acceleration reduced by the acceleration due to non-resonant wave interactions and $m^\star = (A - Z/2)m_0$ is the effective mass. Equation (2) gives $H(O^{6+})/H(He^{2+}) = 0.23$. The difference in the numerical factors in Eqs. (1) and (2) shows that the two different kinematic situations, which have been called "dynamic fractionation" and "static stratification" (Geiss, 1982), could be distinguished by H/He/O measurements at the B-field reversals. Acceleration and expansion in the streamers may well be more complex than indicated in Fig. 1. However, in any case, as shown by our simple estimates, measuring oxygen ions and perhaps other species would not simply provide redundancy, but would add additional, independent constraints on streamer models.

The dynamic fractionation and the static stratification mechanisms both predict local overabundances at some altitude in the corona. In fact, SW expansion models generally lead to low speeds and local enrichment of heavier species in the subsonic regime, quite independent of geometry and model assumptions (cf. Geiss et al., 1970; Bürgi and Geiss, 1986). The existence of such enrichments in

the low corona is confirmed by the high abundances of helium and heavier ions in the "driver gas" that follows flare-generated interplanetary shocks (Hirshberg et al., 1970; Hundhausen, 1972; Galvin et al., 1987, 1993; Ipavich et al., 1986, 1992).

3. Corona Expansion at High Latitude

Extensions of the southern polar coronal hole regularly reached the ecliptic plane during the solar minimum in the 1970s, and thus important characteristics of the SW in HSSTs were established at that time. It was shown, for instance (Bame et al., 1977), that the He/H ratio in the HSSTs, though less less variable than in the slow SW, was still a factor of two below the solar ratio of 0.1. This important finding led to the suggestion that the systematic helium deficit in the SW is to a large part produced in the chromosphere (Geiss 1982). Measurements in flare particle populations by Reames (1994) and others have indirectly shown that the He/O ratio in the low-latitude corona is indeed lower than the solar ratio, which places a further constraint on mechanisms that produce the FIP effect (Sect. 4.).

In 1992 Ulysses, with the Solar Wind Plasma Experiment "SWOOPS" (Bame et al., 1992) and the Solar Wind Ion Spectrometer "SWICS" (Gloeckler et al., 1992) on board, began to pass regularly into and out of the HSST that originates in the Sun's southern coronal hole. In Fig. 3 we present SWICS data for the 13-month period of transition from the slow SW to the HSST, beginning with short excursions into the coronal hole stream and ending with permanent residency in the HSST. An anticorrelation between $T(O^{7+}/O^{6+})$ and solar wind speed is found, confirming that the high speed stream comes from a low-temperature region in the corona, i. e. the southern coronal hole. In Fig. 4 we have drawn the Ulysses trajectory into a sketch that is based on the H-α chart of Carrington rotation 1859, distinguishing times with V_α above or below 600 km/s.

Whereas Fig. 3 shows, by the relatively close correlation between solar wind velocity and $T(O^{7+}/O^{6+})$, that the source region of the HSST is coincident with the coronal hole, Fig. 4 demonstrates – as an example – that the solid angle filled by the HSST in interplanetary space is much larger than the solid angle occupied by the coronal hole right above the solar surface. This has been inferred some time ago from in-ecliptic HSST observations (cf. Kopp and Holzer 1976, Bame 1977, Geiss and Bochsler 1986), but a comparison of the Ulysses data with coronal maps should allow a rather direct estimate of the degree of super-radial expansion which is important for the modelling of high velocity streams. Bürgi and Geiss (1986) solved the momentum equation for a three-fluid plasma with heavier ions as minor components, allowing for super-radial expansion. Using their calculations of solar wind speed and freeze-in temperatures, they confirmed earlier conclusions (e. g. Hollweg 1978) that significant (non-resonant) momentum transfer from waves is needed to bring the low temperature and density conditions in coronal holes into agreement with the high velocities observed in

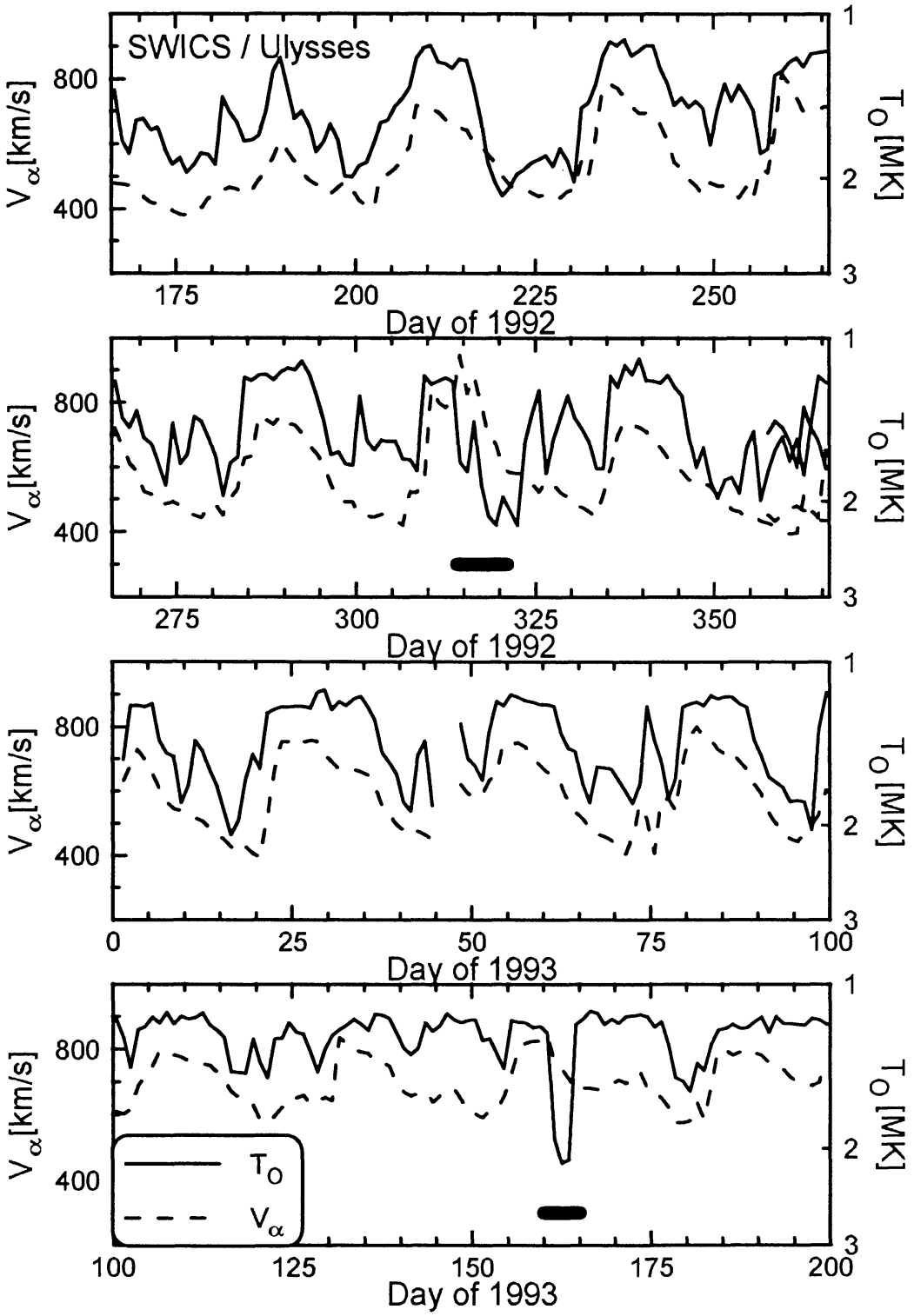

Fig. 3. Recurring transitions of Ulysses between the region with slow SW and the HSST originating in the southern polar corona hole. The SW speed is represented here by the α-speed. T_O, the O^{7+}/O^{6+} freezing-in temperature is drawn inversely for better visualizing the anticorrelation between V_α and T_O. Two periods are marked to indicate CMEs.

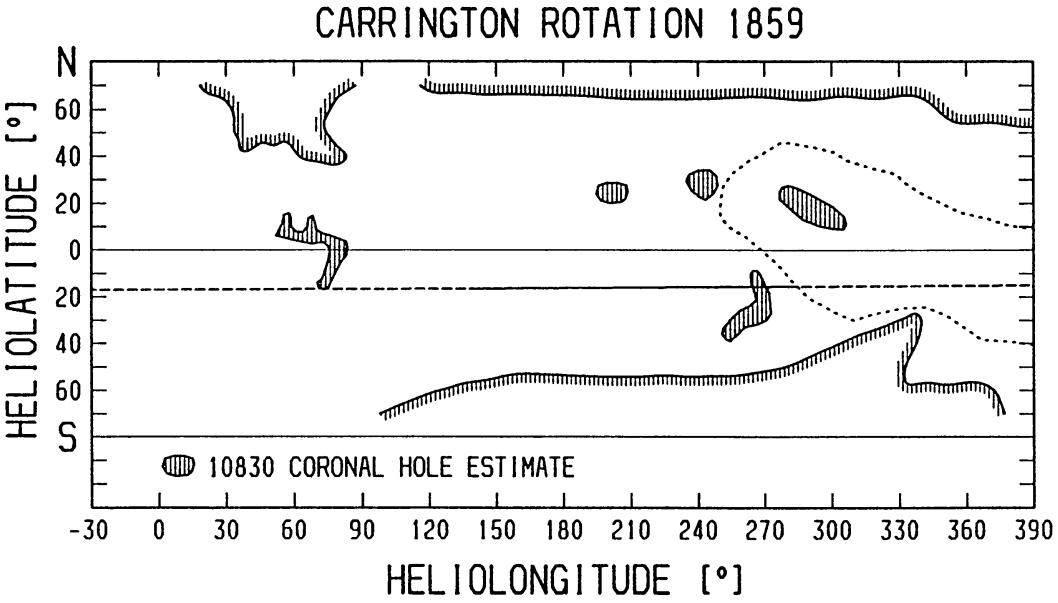

Fig. 4. Ulysses' trajectory (16° to 18° southern latitude) is drawn into the (simplified) H-α map for Carrington Rotation 1859 (NOAA 1992), distinguishing times with α-speed above (solid line) and below (dashed line) 600 km/s. The spacecraft event time was corrected for the difference between the Earth's and Ulysses' solar longitude, as well as for the SW travelling time. The extensions of the large polar coronal holes and some smaller ones are given. The solar activity is increased in the area marked by the dotted line as compared to other areas shown on this map.

the HSSTs.

There is an indication in Fig. 4 of an influence of active regions on the expansion of the coronal hole plasma into interplanetary space: A low SW velocity and high $T(O^{7+}/O^{6+})$ are observed by Ulysses relatively close to the edge of the coronal hole when there is significant activity at mid-latitude (250° to 390° longitude in Fig. 4). On the other hand, a high SW velocity and low $T(O^{7+}/O^{6+})$ are observed at latitudes far away from the edge of the coronal hole when there is no significant activity in the neighbourhood (130° to 240° longitude in Fig. 4). Thorough comparisons of this kind ought to be useful to understand the effects of lateral pressure gradients on the three-dimensional expansion of the corona.

4. Element Fractionation in the Chromosphere: Variation in the FIP Effect

Remote observations and measurements of the SW and of flare particles give a consistent picture of an overabundance of elements with low first ionisation potential (FIP), cf. Meyer (1992): Although there are some significant variations, a basic pattern of this FIP effect has been established: Elements with FIP roughly below 10 eV are overabundant by a factor of about 4 relative to the elements with FIP between $\sim$ 11 eV and 24 eV (cf. Garrard and Stone, 1993; Reames, 1994; Bochsler and Geiss, 1989). On the other hand, helium is underabundant (by a factor of $\sim$ 2) relative to these elements (cf. Geiss, 1982; Meyer, 1992;

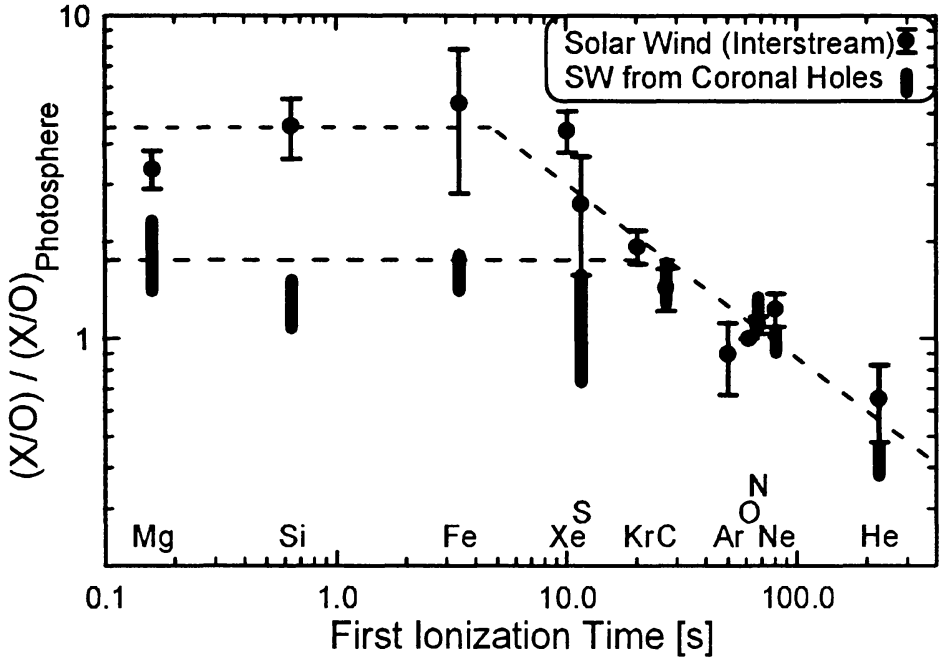

Fig. 5. Elemental abundances in the solar wind as a function of their "first ionisation time" (cf. text). Average patterns in the slow SW and in the HSST are indicated by dashed lines.

Reames, 1994). It was first discovered by investigations of the solar wind plasma in the magnetosheath with the CHEM instrument on AMPTE/CCE that the FIP effect is strongly reduced in fast solar wind streams (Gloeckler et al., 1989; von Steiger et al., 1992; see also the ICI/ISEE-3 results given by Ogilvie et al., 1992). This has been fully confirmed by the SWICS-Ulysses measurements (Galvin et al., 1992; Shafer et al., 1993; von Steiger and Geiss, 1993). It is now evident that the systematic differences between solar abundance and slow SW abundance are largely due to the FIP effect. Temporal or local SW abundance variations are caused in the corona (well documented for the He/H ratio, cf. Neugebauer, 1981), but systematic fractionations produced in the corona are less pronounced than those caused by the FIP effect which operates in the chromosphere. Since the FIP effect is much reduced in the HSSTs, the abundances there are relatively close to the solar abundances (cf. Gloeckler et al., 1989; von Steiger and Geiss, 1994), except probably for helium. Figure 5 shows the difference in the strength of the FIP effect between slow SW and HSST. The FIP effect does not produce a simple, monotonic relation of element abundances versus first ionisation potential which is most explicitly evident from the solar wind abundances of Kr and Xe derived from the gases trapped in lunar soils (Wieler et al., 1993). Geiss and Bochsler (1985) and von Steiger and Geiss (1989) have calculated ionisation times of various elements for zero optical depth at the solar surface. If we plot the elemental abundances as a function of these "first ionisation times (FIT)", we obtain rather well defined, nearly monotonous relationships clearly showing

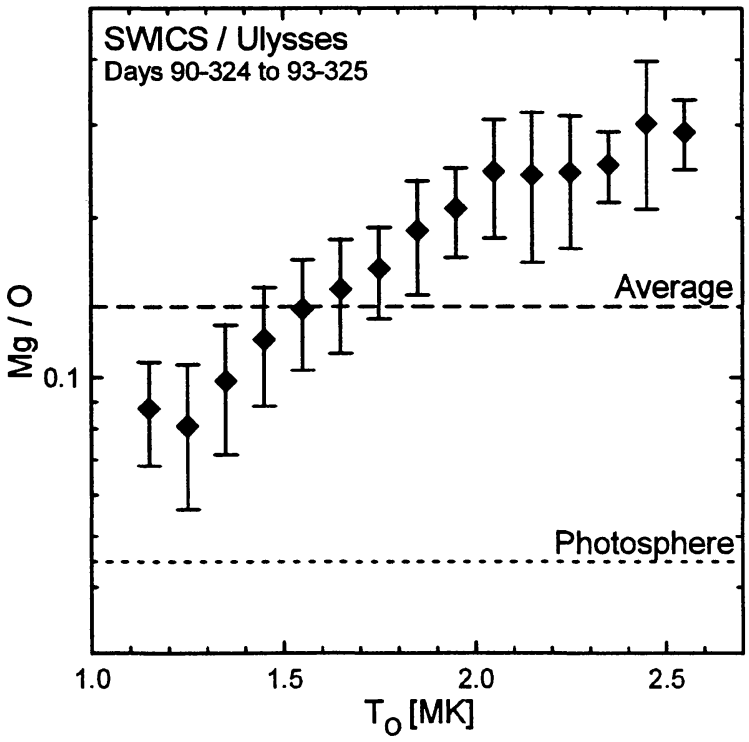

Fig. 6. The Mg/O ratio as a function of T_O, the freezing-in temperature $T(O^{7+}/O^{6+})$. Given are standard deviations (not standard errors, which would be much smaller).

the difference between slow SW and HSST (Fig. 5). These observations constitute important constraints for mechanisms that are designed to explain the FIP effect (cf. the discussions by Meyer, 1992; von Steiger and Geiss, 1994; Geiss, Gloeckler and von Steiger, 1994).

Oxygen and magnesium are a pair of a high- and a low-FIP element that can be particularly well studied with SWICS-Ulysses. The Mg/O ratio is found to decrease with increasing SW speed which reflects the weakening of the FIP effect in the HSST. However, the correlation is much weaker than the correlation between the Mg/O ratio and the freezing-in temperature $T(O^{7+}/O^{6+})$ shown in Fig. 6. This points to a relationship between coronal conditions and structure or processes in the chromosphere, which we shall further explore in the next section.

5. Relation between Chromospheric and Coronal Processes

We have used a superposed epoch method for studying systematics in the variations of solar wind properties across the border between the slow solar wind and the HSST during the period day 191.1992 to day 098.1993) when Ulysses spent similar times in the slow solar wind and in the HSST. One solar rotation (days 308–334.1992) was omitted, because a CME occurred. Using V_α = 600 km/s crossings as markers we empirically determined the average period of a full cycle (t = 25.8 days) and its increase with time (0.08 days per full cycle). As Ulysses flew to higher latitude and solar activity decreased, the partitioning of t

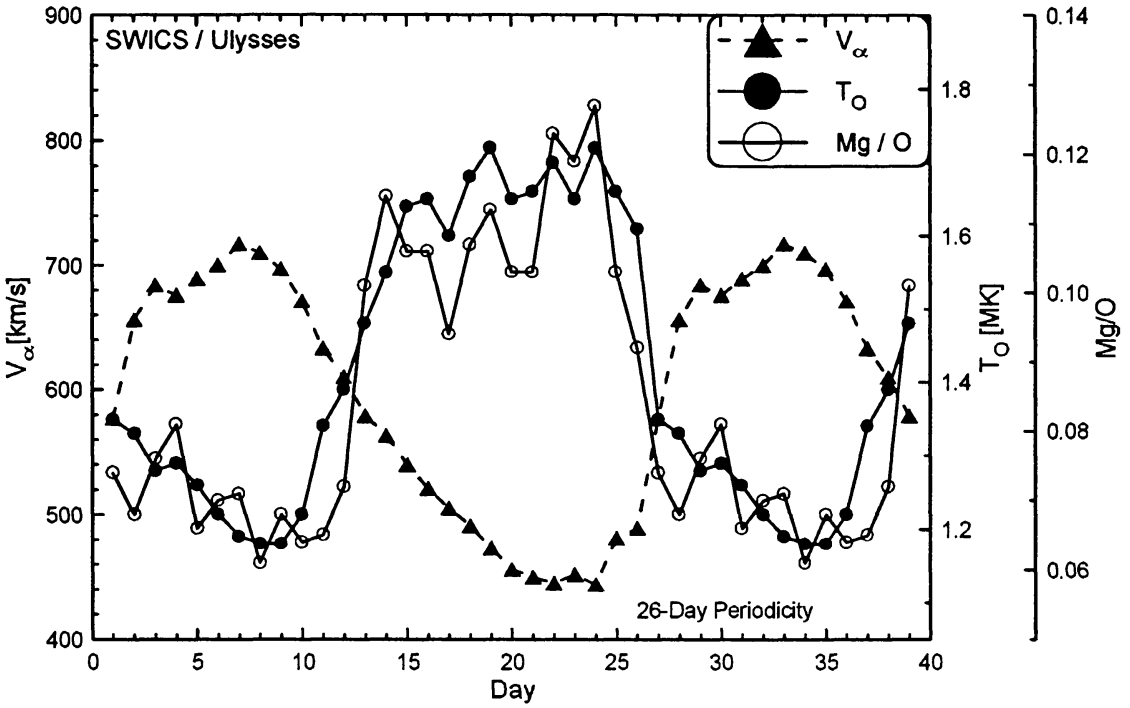

Fig. 7. Superposed epoch plot showing the systematic variations during the (effective) solar rotation period. The procedure used is outlined in the text. $T(O^{7+}/O^{6+})$ and Mg/O vary very steeply and trace each other almost perfectly, indicating a close relationship between corona temperature and chromospheric structure or processes.

between slow SW and HSST changed with time. Although this change is very irregular (cf. Fig. 3), we used a simple linear increase of 0.34 days per full cycle for the fraction of time in the HSST (determined again on the basis of the V_α = 600 km/s crossings). The data taken were our standard daily averages. The systematic changes in period and in fraction of time in and outside the HSST were taken into account by omitting or adding days with a random number method. Only 6% of the days were affected by this adjustment procedure. We have deliberately chosen this crude but straightforward procedure, which uses the minimum number of parameters, in order to avoid an inadvertent introduction of biases. A more refined procedure might improve, but certainly not destroy the systematics we find.

In Fig. 7 we show the result for three parameters: Plotted are, as a function of epoch-time, the solar wind speed (represented by the α-speed), coronal temperature (represented by $T(O^{7+}/O^{6+})$) and the strength of the FIP effect (represented by the Mg/O ratio). The resulting diagramme shows several remarkable features:

1. $T(O^{7+}/O^{6+})$ and the Mg/O ratio follow each other very closely, their relation to V_α is not as tight. This is of course consistent with the correlation shown in Fig. 6.
2. The figure indicates that even the fine variations of $T(O^{7+}/O^{6+})$ and Mg/O are correlated in the slow SW, but not so much in th HSST. As Ulysses

proceeds further into the southern coronal hole we should be able to further study variations in HSST abundances (or their absence).

3. The transition between low and high is very steep for $T(O^{7+}/O^{6+})$ and Mg/O. Statistical analyses show that it is almost as steep as a step function would be, when subjected to our procedure. Thus chromosphere and corona have a common, relatively sharp boundary, separating the low- from the high-FIP region in the chromosphere and the low- from the high-temperature region in the corona. This points to a causal relationship of the kind that conditions inside or even below the chromosphere determine the supply of energy into the corona, and underlines that discussions of the origin of the solar wind will have to include chromospheric processes.
4. The SW speed as a function of epoch-time shown in Fig. 7 with the characteristically slow decline of the speed in the trailing edge is similar to the pattern found by Bame et al. (1977) in the ecliptic during the solar minimum in the mid 1970s. When the trailing edge of a high speed stream is mapped back to the corona, it becomes clear, as shown by Nolte et al. (1977), that the large range of decreasing velocities comes from a relatively restricted range in longitude. This implies that the boundary between low and high $T(O^{7+}/O^{6+})$ and Mg/O at the eastern rim of the coronal hole is even sharper than is indicated in Fig. 7.
5. The HSST and the adjacent slow SW are embedded in interplanetary field-line configurations which do not seem to be grossly different. What causes then the reduction in kinetic energy by a factor of 4? More abundant closed magnetic field lines in the lower corona, weaker wave intensities or the reduced parallel component of the gravitational force might be factors worth exploring. Inclusion of other solar wind parameters into the superposed epoch analysis of Fig. 7 might help to understand why solar wind acceleration becomes less effective just outside the coronal holes.

Acknowledgements

The authors thank H. Balsiger, A. Bürgi, A. B. Galvin, and R. Wimmer for discussions. This work was supported by the Swiss National Science Foundation and by the US National Aeronautics and Space Administration (NASA/JPL contract 955460).

References

Bame, S.J., Asbridge J.R., Feldman W.C., and Gosling J.T.: 1977, *J. Geophys. Res.* **82**, 1487

Bame, S.J., et al.: 1992, *Astron. Astrophys. Suppl. Ser.* **92**, 237

Bochsler, P. and Geiss, J.: 1989, in J.H. Waite Jr., ed(s)., *Solar System Plasma Physics*, Geophysical Monograph 54, 133

Borrini, G., Gosling, J.T., Bame, S.J., Feldman, W.C., and Wilcox, J.M.: 1981, *J. Geophys. Res.* **86**, 4565

Bürgi, A.: 1992, in E. Marsch and R. Schwenn, ed(s)., *Solar Wind Seven*, Pergamon Press: Oxford, 333
Bürgi, A. and Geiss, J.: 1986, *Solar Physics* **103**, 143
Galvin, A.B., et al.: 1987, *J. Geophys. Res.* **92**, 12069
Galvin, A.B., Ipavich, F.M.,Gloeckler, G., von Steiger, R., and Wilken, B.: 1992, in E. Marsch and R. Schwenn, ed(s)., *Solar Wind Seven*, Pergamon Press: Oxford, 337
Galvin, A.B., Gloeckler, G., Ipavich, F.M., Shafer, C.M., Geiss, J., and Ogilvie, K.W.: 1993, *Adv. Space Res.* **13**, (6)75
Garrard, T.L., and Stone, E.C.: 1993, in *Proc. 23. Int. Cosmic Ray Conf.*
Geiss, J.: 1982, *Space Sci. Rev.* **33**, 201
Geiss, J.: 1985, in *Future Missions in Solar, Heliospheric and Space Plasma Physics*, ESA SP-235, 37
Geiss, J., Hirt, P., and Leutwyler, H.: 1970, *Solar Physics* **12**, 458
Geiss, J., and Bochsler, P.: 1985, in *Rapports isotopiques dans le système solaire*, Cepadues-editions: Toulouse, 213
Geiss, J., Gloeckler, G., and von Steiger, R.: 1994, in *Proc. Royal Society Symp. on the Solar System*, London, in press
Geiss, J., and Bochsler, P.: 1986, in R.G. Marsden, ed(s)., *The Sun and the Heliosphere in Three Dimensions*, Reidel: Dordrecht, 173
Gloeckler, G., Ipavich, F.M., Hamilton, D.C., Wilken, B. and Kremser, G.: 1989, *EOS Trans. AGU* **70**, 424
Gloeckler, G., and Geiss, J.: 1989, in C.J. Waddington, ed(s)., *Proc. Cosmic Abundances of Matter Symp.*, AIP Conf. Proc. **183**, 71
Gloeckler, G., et al.: 1992, *Astron. Astrophys. Suppl. Ser.* **92**, 267
Hirshberg, J., Asbridge, J.R., and Robbins, D.E.: 1972, *J. Geophys. Res.* **77**, 3583
Hollweg, J.V.: 1974, *J. Geophys. Res.* **79**, 1539
Hollweg, J.V.: 1978, *Rev. Geophys. Space Phys.* **16**, 689
Hundhausen, A.J.: 1972, *Solar Wind and Coronal Expansion*, Springer: New York
Ipavich, F.M., et al.: 1986, *J. Geophys. Res.* **91**, 4133
Ipavich, F.M., Galvin, A.B., Geiss, J., Ogilvie, K.W., and Gliem, F.: 1992, in E. Marsch and R. Schwenn, ed(s)., *Solar Wind Seven*, Pergamon Press: Oxford, 369
Kopp, R.A., and Holzer, T.E.: 1976, *Solar Phys* **49**, 43
Krieger, A.S., Timothy, A.F. and Roelof, E.C.: 1973, *Solar Phys* **29**, 505
Meyer, J.P.: 1992, in N. Prantzos, E. Vangioni-Flam and M. Cassè, ed(s)., *Origin and Evolution of the Elements*, Cambridge University Press, 26
NOAA: 1992, *Prelim. Report and Forecast of Solar Geophys. Data*, NOAA: Boulder
Noci, G., and Porri, A.: 1983, in *IAGA 18th Gen. Ass., Hamburg*, paper 4L.04
Nolte, J.T., Krieger, A.S., Roelof, E.C., and Gold, R.E.: 1977, *Solar Phys.* **51**, 459
Neugebauer, M.: 1981, *Fundamentals of Cosmic Physics* **7**, 131
Ogilvie K.W., Coplan M.A. and Geiss J.: 1992, in E. Marsch and R. Schwenn, ed(s)., *Solar Wind Seven*, Pergamon Press: Oxford, 379
Parker, E.N.: 1960, *Astrophys. J.* **132**, 821
Parker, E.N:: 1963, *Interplanetary Dynamical Processes*, Interscience: New York
Reames, D.V.: 1994, *Adv. Space Res.* **14**, (4)177
Shafer, C.M., Gloeckler, G., Galvin, A.B., Ipavich, F.M., Geiss, J., von Steiger, R., and Ogilvie, K.W.: 1993, *Adv. Space Res.* **13**, (6)79
Schmid, J., Bochsler, P., and Geiss, J.: 1988, *Astrophys. J.* **122**, 181
Schwenn, R., and Marsch, E. (eds.): 1990, *Physics of the Inner Heliosphere*, Springer: Heidelberg
von Steiger, R., Christon, S.P., Gloeckler, G., and Ipavich, F.M.: 1992, *Astrophys. J.* **389**, 791
von Steiger, R., and Geiss, J.: 1989, *Astron. and Astrophys.* **225**, 222
von Steiger, R., and Geiss, J.: 1993, *Adv. Space Res.* **13**, (6)63
von Steiger, R., and Geiss, J.: 1994, in J.R. Jokipii, C.P. Sonnett, and M.S. Giampapa, ed(s)., *Cosmic Winds and the Heliosphere*, University of Arizona Press: Tucson, in press
Wang, A.H., Wu, S.T., Suess, S.T., and Poletto, G.: 1993, *Solar Phys.* **147**, 55
Wieler, R., Baur, H., and Signer, P.: 1993, *Proc. Lunar and Planet. Sci.* **24**, 1519